

# A *Chandra* Survey of Milky Way Globular Clusters II: Testing the Hills-Heggie Law

Zhongqun Cheng<sup>1,2,3</sup>, Zhiyuan Li<sup>2,3</sup>, Xiaojie Xu<sup>2,3</sup>, Xiangdong Li<sup>2,3</sup>, Zhenlin Zhu<sup>2,3</sup> and Taotao Fang<sup>1</sup>

<sup>1</sup> *Department of Astronomy and Institute for Theoretical Physics and Astrophysics, Xiamen University, Xiamen, Fujian 361005, China*

<sup>2</sup> *School of Astronomy and Space Science, Nanjing University, Nanjing 210023, China*

<sup>3</sup> *Key Laboratory of Modern Astronomy and Astrophysics (Nanjing University), Ministry of Education, Nanjing 210023, China*

lizy@nju.edu.cn; lixd@nju.edu.cn; fangt@xmu.edu.cn

## ABSTRACT

Binary-single and binary-binary encounters play a pivotal role in the evolution of star clusters, as they may lead to the disruption or hardening of binaries, a novel prediction of the Hills-Heggie law. Based on our recent *Chandra* survey of Galactic globular clusters (GCs), we revisit the role of stellar dynamical interactions in GCs, focusing on main-sequence (MS) binary encounters as a potential formation channel of the observed X-ray sources in GCs. We show that the cumulative X-ray luminosity ( $L_X$ ), a proxy of the total number of X-ray-emitting binaries (primarily cataclysmic variables and coronally active binaries) in a given GC, is highly correlated with the MS binary encounter rate ( $\Gamma_b$ ), as  $L_X \propto \Gamma_b^{0.77 \pm 0.11}$ . We further test the Hills-Heggie law against the *binary hardness ratio*, defined as the relative number of X-ray-emitting hard binaries to MS binaries and approximated by  $L_X/(L_K f_b)$ , with  $L_K$  being the GC K-band luminosity and  $f_b$  the MS binary fraction. We demonstrate that the binary hardness ratio of most GCs is larger than that of the Solar neighborhood stars, and exhibits a positive correlation with the cluster specific encounter rate ( $\gamma$ ), as  $L_X/(L_K f_b) \propto \gamma^{0.65 \pm 0.12}$ . We also find a strong correlation between the binary hardness ratio and cluster velocity dispersion ( $\sigma$ ), with  $L_X/(L_K f_b) \propto \sigma^{1.71 \pm 0.48}$ , which is consistent with the Hills-Heggie law. We discuss the role of binary encounters in the context of the Nuclear Star Cluster, arguing that the X-ray-emitting, close binaries detected therein could have been predominately formed in GCs that later inspiralled to the Galactic center.

*Subject headings:* binaries: close — X-rays: binaries — globular clusters: general — Galaxy: center — stars: kinematics and dynamics

## 1. Introduction

X-ray observations in the 1970s have discovered a strong over-abundance of outbursting low-mass X-ray binaries (LMXBs) in globular clusters (GCs) with respect to the Galactic field (Clark 1975; Katz 1975), which quickly stimulated the discussions of stellar dynamical interactions as an effective formation channel of LMXBs in GCs. Widely accepted scenarios include: tidal capture of neutron star (NS) by main sequence (MS) stars (Fabian et al. 1975), collision of NS with giant stars (Sutantyo 1975), and exchange encounter of NS with primordial binaries (Hills 1976). All these mechanisms have a similar dependence on the rate of stellar close encounters in

GCs, which can be expressed as  $\Gamma \propto \int \rho^2 / \sigma$ , with  $\rho$  the stellar density and  $\sigma$  the velocity dispersion. Given  $\Gamma$ , one can readily predict the probability of finding LMXBs in GCs of the Milky Way or external galaxies (Verbunt & Hut 1987; Jordán et al. 2004; Sivakoff et al. 2007; Jordán et al. 2007; Peacock et al. 2009).

Studies of stellar dynamical interactions in the 1970s and 1980s also predicted a possible formation mechanism of close binaries in GCs, namely, the binary-single (*b-s*) and binary-binary (*b-b*) encounters (Hills 1975; Heggie 1975; Hoffer 1983; Mikkola 1983, 1984a,b; Hut et al. 1992a,b; Hut 1993; Bacon et al. 1996). Due to energy equipar-

tition, stars involved in these interactions tend to have the same kinetic energy, which will change the bound energy of the binary and lead to expansion or contraction of the binary orbit. Generally, the evolution of binary orbits in dynamical encounters are dictated by the Hills-Heggie law: hard binaries (with bound energy  $|E_b|$  larger than the kinetic energy  $E_k$  of the intruding star) tend to be harder, while soft binaries ( $|E_b| < E_k$ ) tend to be softer and eventually be disrupted (Hills 1975; Heggie 1975; Hut 1993).

For the numerous MS binaries in GCs, the Hills-Heggie law provides an effective mechanism for transforming them into exotic binaries, which has been confirmed by numerical simulations. For example, the exchange encounters of MS binaries with compact objects may lead to the formation of cataclysmic variables (CVs) or LMXBs (Heggie et al. 1996; Rasio et al. 2000; Ivanova et al. 2006, 2008). In the case of no exchange, the MS binaries of short orbital periods may evolve toward tidal locking between stellar rotation and orbital motion, effectively enhancing the stellar magnetic activities and transforming them into coronally active binaries (ABs). Meanwhile, enhancing the rate of binary mass transfer or merger can lead to the formation of blue stragglers (Hut et al. 1992a; Fregeau et al. 2004; Chatterjee et al. 2013).

On the observational side, the *Chandra X-ray Observatory* has revealed numerous weak X-ray sources (with luminosities  $\lesssim 10^{34}$  erg s $^{-1}$ ) in GCs, the majority of which are found to be CVs and ABs, with a small addition of quiescent LMXBs and millisecond pulsars (MSPs) (see Heinke 2010 for a recent review). All these systems are close binaries. Pooley et al. (2003) were among the first to suggest that these sources are dynamically originated, based on the observed correlation between the number of detected X-ray sources ( $N_X$ ) and  $\Gamma$  in a sample of Galactic GCs. It is noteworthy that the  $N_X - \Gamma$  correlation was found to be sub-linear<sup>1</sup>, which suggests a lower formation efficiency of weak X-ray sources in more massive GCs (with higher  $\Gamma$ ).

Based on archival *Chandra* observations, we have recently carried out an X-ray survey of 69 Galactic GCs (Cheng et al. 2018, hereafter Paper I). Using the cumulative X-ray luminosity ( $L_X$ ) as a proxy of the weak X-ray source populations, we have shown that  $L_X$  is highly correlated with not only  $\Gamma$ , but also the cluster mass ( $M$ ), suggesting that the primordial channel of close binary formation is not negligible. In the meantime, our larger GC sample dis-

approves a positive correlation between the source abundance (approximated by  $L_X/L_K$ , where  $L_K$  is the GC K-band luminosity, itself a good proxy of the cluster mass; Paper I) and the specific encounter rate,  $\gamma = \Gamma/M$ , which was originally suggested by Pooley & Hut (2006). Furthermore, we demonstrated that the weak X-ray sources (mainly CVs and ABs) are under-abundant in GCs with respect to the field, a behavior opposite to the LMXBs and MSPs (see also Xu & Li (2018) for the case of M31 GCs). These findings render the dynamical origin of GC weak X-ray sources far from conclusive.

The problem may lie in the ambiguity of the stellar dynamical interactions collectively expressed by the parameter  $\Gamma$ . In particular, when considering the formation of close binaries in a dense stellar environment such as GCs, there exist two competing dynamical processes: single-single (*s-s*) encounters (tidal capture, direct collision, etc.) that usually lead to the dissipation of stellar kinetic energy and result in the formation of binaries, while *b-s* and *b-b* encounters tend to modify or destroy binaries, leading to a gradual net decrease of binary abundance (Hills 1975; Heggie 1975; Mikkola 1983, 1984a,b; Hut et al. 1992a,b; Hut 1993). For CVs and ABs, the binary-relevant encounters are non-negligible, because their progenitor MS binaries are mainly low-mass stars, which will evolve on a timescale comparable to or even greater than the GC relaxation time.

According to the Hills-Heggie law, the evolution of MS binaries in GCs depends on the average kinetic energy  $E_k$  of the intruding star, which is related to the stellar velocity dispersion as  $E_k \sim \sigma^2$ . There exists a watershed orbital separation ( $a_w$ ) for the MS binaries, with  $E_b = GM_*^2/2a_w \sim E_k$ , and hence  $a_w \propto \sigma^{-2}$ . For MS binaries with an orbital separation greater than  $a_w$ , they are more likely to be disrupted by *b-s* encounters, and to a lesser extent, by *b-b* encounters (see below). Otherwise, the MS binaries will be dynamically transformed into close binaries and ultimately become ABs or CVs. The prediction of dynamical disruption of binaries has been confirmed by the observed anti-correlation between MS binary fraction ( $f_b$ ) and  $\sigma$  in GCs (Milone et al. 2012), and is also supported by the abnormally low values of  $f_b$  in the core of some clusters (de Grijs et al. 2013).

On the other hand, the effect of dynamical hardening of binaries in GCs, as also predicted by the Hills-Heggie law, remains to be tested. We aim to provide a statistical test of this effect in the present work. In Section 2, we first introduce the binary-relevant encounter rate ( $\Gamma_b$ ), and estimate their importance relative to the single-single encounter rate

<sup>1</sup>The logarithmic slope of the  $N_X - \Gamma$  relation in Pooley et al. (2003) is  $0.74 \pm 0.36$ , which has been revised as  $0.55 \pm 0.09$  in Maxwell et al. (2012).

( $\Gamma_s$ ) in GCs. In Section 3, we explore the formation of weak X-ray sources in GCs according to the binary encounter scenario. In Section 4, we test the Hills-Heggie law in the scope of binary hardening in GCs. In Section 5, we discuss the role of binary encounters in the context of X-ray sources in the Nuclear Star Cluster. Concluding remarks are provided in Section 6.

## 2. Binary-single encounter rate

To compare the two competing dynamical processes in GCs, we estimate the  $s$ - $s$  and  $b$ - $s$ / $b$ - $b^2$  encounter rates separately, which are defined as an integration over the cluster volume (Verbunt 2003):

$$\Gamma_s \propto \int n_s^2 A_s v dV \propto \int \frac{n_s^2 R_*}{v} dV, \quad (1)$$

$$\Gamma_b \propto \int n_b n A_b v dV \propto \int \frac{n_b n a}{v} dV, \quad (2)$$

where  $n_s$  ( $n_b$ ) is the number density of single stars (MS binaries),  $n = n_s + n_b$ , and  $A_s$  ( $A_b$ ) the encounter cross-section, which is proportional to the stellar radius  $R_*$  (binary orbital separation  $a$ ) and inversely proportional to the square of relative velocity  $v$  (Davies 2002). Generally, the relative velocity  $v$  can be characterized by the stellar velocity dispersion  $\sigma$ . The density of MS binaries ( $n_b$ ) can be related to the observed binary fraction  $f_b$ , with  $f_b = n_b/n$ , while the stellar density  $n$  can be approximated by the stellar luminosity density,  $\rho = n\langle L \rangle$ , where  $\langle L \rangle$  is the characteristic luminosity of MS stars. Now, Equations (1) and (2) can be rewritten as:

$$\Gamma_s \propto \int \frac{(1 - f_b)^2 \rho^2 R_*}{\sigma} dV, \quad (3)$$

$$\Gamma_b \propto \int \frac{f_b \rho^2 a}{\sigma} dV. \quad (4)$$

To accurately calculate  $\Gamma_s$  and  $\Gamma_b$ , a robust measurement of the radial stellar density profile  $\rho(r)$  and binary fraction profile  $f_b(r)$  is needed. However, due to the low intrinsic luminosities and crowded stellar environment, the identification of MS binaries in GCs is challenging. Consequently, accurate measurements of  $f_b$  and  $a$  as a function of distance from the cluster center are currently absent (Sollima et al. 2007; Milone et al.

2012; Ji & Bregman 2015). Therefore, we estimate  $\Gamma_s$  and  $\Gamma_b$  by considering a global  $f_b$  for a given GC, and take  $R_*$  and  $a$  as constants throughout the cluster<sup>3</sup>. Equations (3) and (4) can then be further simplified as  $\Gamma_s \propto (1 - f_b)^2 \times \Gamma$  and  $\Gamma_b \propto f_b \times \Gamma$ , respectively. By choice, both  $f_b$  and  $\Gamma$  are global parameters and are more compatible with the GC cumulative X-ray luminosity as measured in Paper I.

To find out the dominant type of encounters<sup>4</sup>, we estimate the ratio of the two competing dynamical interactions with Equations (3) and (4):

$$\frac{\Gamma_b}{\Gamma_s} \sim \frac{f_b}{(1 - f_b)^2} \frac{a}{R_*}. \quad (5)$$

Considering a distribution of MS binary orbital period ranging from  $\sim 10 - 5000$  days<sup>5</sup>, we have values of  $a/R_*$  ranging from 30 to 1900 for a typical MS mass of  $0.8 M_\odot$ . The observed binary fraction  $f_b$  in most GCs ranges from 1% to 20% (Milone et al. 2012), thus the ratio  $\Gamma_b/\Gamma_s$  ranges from 0.3 to 600. Since most MS binaries have been dynamically exhausted in GCs and the present-day  $f_b$  is smaller than it used to be, the ratio of  $\Gamma_b/\Gamma_s$  should be even larger in the past. Moreover, due to mass segregation, MS binaries are more likely to sink to the cluster core and thus subject to higher encounter rates than single stars. Such an effect has been ignored in Equation (5), but otherwise would enhance the value of  $\Gamma_b/\Gamma_s$ . Therefore, the  $b$ - $s$ / $b$ - $b$  encounters dominate over the  $s$ - $s$  encounters in GCs. In the following, we will focus on the binary-relevant encounters when considering the formation of weak X-ray sources.

## 3. Formation of hard X-ray binaries by binary-single encounters

Among the 69 GCs studied in Paper I, thirty, including 6 core-collapsed GCs and 24 dynamically normal GCs, have a measured MS binary fraction

<sup>3</sup>The radii of low mass MS stars should have a narrow range, but the size of binaries may vary by orders of magnitude, which will lead to an overestimate of  $\Gamma_b$  in core-collapsed GCs. See Section 3 for further discussions.

<sup>4</sup>The ratio of the  $b$ - $s$  and  $b$ - $b$  encounters can be estimated with  $\Gamma_{bs}/\Gamma_{bb} \sim (n_b n_s A_b)/(n_b n_b A_b) \sim (1 - f_b)/f_b$ . The  $b$ - $s$  encounters dominate over  $b$ - $b$  encounters in GCs:  $\Gamma_{bs}/\Gamma_{bb}$  ranges from 4 to 99 when  $f_b$  ranges from 1% to 20% (Milone et al. 2012).

<sup>5</sup>According to Equation (1) of Hut et al. (1992b), binaries with orbital period less than  $\sim 10$  days may suffer from no strong encounters in typical GCs with  $\rho_c \sim 10^4 M_\odot \text{pc}^{-3}$  and age of  $\sim 10$  Gyr. On the other hand, for a GC with stellar velocity dispersion  $\sigma \sim 10 \text{ km s}^{-1}$ , the watershed orbital separation  $a_w$  corresponds to a watershed orbital period  $\sim 5000$  days, provided that the constituent stars have masses of  $\sim 0.8 M_\odot$ .

<sup>2</sup>Here we make no distinction between the  $b$ - $b$  and  $b$ - $s$  encounters, since both of them obey the Hill-Heggie law and have a similar effect on modifying binaries (Mikkola 1983, 1984a,b; Bacon et al. 1996). See also Footnote 5 below.

( $f_b$ ) from Milone et al. (2012). Using the method outlined in Section 2, we calculate the MS binary encounter rate for each of these 30 GCs. We adopt the total encounter rate by Bahramian et al. (2013), which was calculated as  $\Gamma = 4\pi\sigma_c^{-1} \int \rho^2(r)r^2 dr^6$  and normalized to a reference value of 1000 for NGC 104. Thus the binary-related encounter rate of NGC 104 is  $\Gamma_b = 180_{-65}^{+66}$ , for its MS binary fraction  $f_b = (1.8 \pm 0.6)\%$ . The relative errors of  $f_b$  and  $\Gamma$  in most GCs are  $\lesssim 30\%$  (Table 1), which have been included in the error budget of  $\Gamma_b$  through standard error propagation.

Figure 1a displays the GC X-ray luminosity versus  $\Gamma_b$ . The values of  $L_X$  were adopted from Paper I. GCs of solid detections are shown by filled symbols (with 68% uncertainties), while X-ray non-detected GCs are denoted by open symbols representing the 95% upper limit. For the dynamically normal GCs, there is a significant correlation between  $L_X$  and  $\Gamma_b$ , with Spearman's rank correlation coefficient  $r = 0.902$  and random correlation p-value  $p \ll 0.0001$ . We fit the relation with a power-law function, which is plotted as the purple line in Figure 1a, with  $L_X \propto \Gamma_b^{0.77 \pm 0.11}$ .

We note that in Paper I, a strong correlation between  $L_X$  and  $\Gamma$  has also been found for the full sample of dynamically normal GCs, with  $L_X \propto \Gamma^{0.79 \pm 0.12}$ . Here, for the subset of dynamically normal GCs selected in Figure 1a, the correlation between  $L_X$  and  $\Gamma$  is also significant, with the Spearman's correlation coefficient  $r = 0.896$  and random correlation p-value  $p \ll 0.0001$ . However, we argue that  $\Gamma_b$  be more fundamental than  $\Gamma$  in describing the origin of the weak X-ray sources in GCs. First, as discussed in Section 2, the typical value of  $\Gamma_b/\Gamma_s$  is much larger than unity in GCs, and the encounters evaluated in  $\Gamma$  are actually dominated by  $\Gamma_b$ . Moreover, the sublinear relation of  $L_X$ – $\Gamma$  can be understood as due to binary-related encounters. This is because stars in more massive GCs will be more energetic ( $E_k \propto \sigma^2$ ), thus more MS binaries will be dynamically disrupted rather than be transformed into X-ray-emitting close binaries. As a result, formation of weak X-ray sources is less efficient in massive GCs than in low-mass clusters, as evidenced by an anti-correlation between the GC X-ray emissivity and cluster mass<sup>7</sup>,  $\epsilon_X \equiv L_X/M \propto M^{-0.30 \pm 0.11}$  (Paper I).

The core-collapsed GCs in Figure 1a deserve some

remarks. These clusters appeared to be abundant in X-ray sources according to the  $N_X$  –  $\Gamma$  relation of Pooley et al. (2003), however, with the updated  $\Gamma$ , Bahramian et al. (2013) found a paucity of X-ray sources in these clusters. The binary encounter scenario provides an explanation for these clusters: due to the much older dynamical age, MS binaries in core-collapsed GCs are on average much harder than those in dynamically normal GCs (Figure 2). Thus, taking the binary orbital separation  $a$  as a constant in Equation (4) could have led to an overestimated  $\Gamma_b$  for these GCs (e.g., NGC 362 and NGC 6681 as denoted in Figure 1a).

In Figure 1a, we also include the case of the Nuclear Star Cluster (NSC) for comparison. The vast majority of the weak X-ray sources (with luminosities spanning  $10^{31} - 3 \times 10^{33} \text{ erg s}^{-1}$ ) detected in the NSC are thought to be CVs (Zhu et al. 2018). The cumulative X-ray luminosity of the NSC is estimated from the X-ray source catalog of Zhu et al. (2018), as follows. From the accumulated spectrum of the sources detected within a galactocentric radius  $r < 100''$ , we derive an unabsorbed luminosity of  $3.3 \times 10^{34} \text{ erg s}^{-1}$  in 0.5–8 keV band. As shown in Zhu et al. (2018), these sources account for a resolved fraction of  $\sim 24\%$ . Therefore, we adopt  $1.37 \times 10^{35} \text{ erg s}^{-1}$  as a firm upper limit of the cumulative luminosity of all weak X-ray sources in the NSC. To estimate the encounter rate of the NSC, we follow the procedure of Bahramian et al. (2013) and numerically integrate  $\rho^2(r)/\sigma(r)$  throughout the NSC and NGC 104, the latter serving as a norm here. We have adopted the stellar density and velocity dispersion profiles as determined by Fritz et al. (2016) for the NSC, the cumulative stellar mass of which within was estimated to be  $(6.09 \pm 0.97) \times 10^6 M_\odot$  within  $r < 100''$  (Table 1). For the reference value of  $\Gamma = 1000$  for NGC 104, we obtain  $\Gamma = 25600 \pm 7700$  for the NSC. Since the MS binary fraction of the NSC is currently poorly constrained, we assume two plausible values of  $f_b = 1\%$  and  $10\%$ <sup>8</sup>, which results in  $\Gamma_b$  ranging from 2560 and 25600. From Figure 1a, it can be seen that the NSC is compatible with the relation defined by the GCs. The implication of this finding will be addressed in Section 5.

As shown in Paper I, the cumulative GC X-ray luminosity may be related to the number ( $N_X$ ) of the weak X-ray sources,  $L_X = N_X \bar{L}_X$ , and the abundance of weak X-ray source can be expressed as,

$$L_X/L_K = f_b(N_X/N_b)(\bar{L}_X/\bar{L}_K), \quad (6)$$

where  $L_K$  is the GC cumulative K-band luminosity,

<sup>6</sup>Here the distribution of  $\sigma(r)$  was assumed to be flat, with a value equivalent to the cluster central velocity dispersion  $\sigma_c$ . Such a simplification is reasonable, since the profile of  $\sigma(r)$  is much flatter than  $\rho(r)$  in GCs.

<sup>7</sup>This anti-correlation has been confirmed by Xu & Li (2018) with 44 GCs in M31.

<sup>8</sup>Such a range of  $f_b$  is theoretically predicted by numerical simulations considering binary evolution in the NSC (see Appendix C of Genozov et al. (2018) for details).

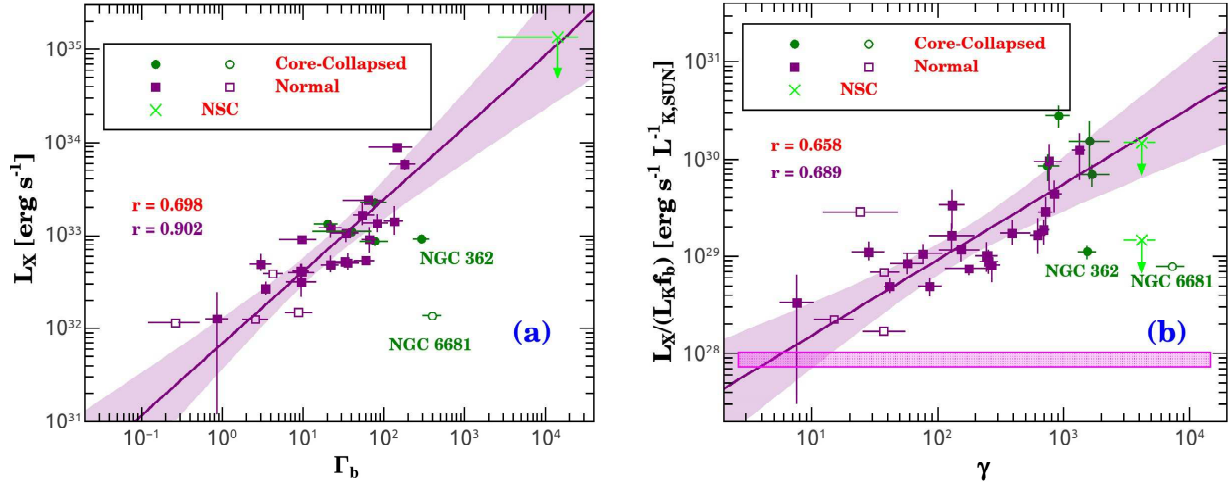


Fig. 1.— (a): GC X-ray luminosity as a function of the MS binary encounter rate; (b):  $L_X/(L_K f_b)$  as a function of the specific encounter rate  $\gamma$ . The olive circles and purple squares denote the core-collapsed and dynamically normal GCs, with filled and open symbols represent the actual detection and the upper limit (at 95% confidence). The green crosses mark the upper limits of thbinaries) in the Nuclear Star Cluster, and  $L_X/(L_K f_b)$  in (b) were calculated with  $f_b = 1\%$  and  $f_b = 10\%$  separately. The purple and red text indicates the Spearman’s rank correlation coefficient of the dynamically normal and total GCs, respectively. The purple solid line is the best-fitting function for dynamically normal GCs (GCs with upper limit were not included in the fit), and the shaded area represents the 95% confidence interval. Magenta strip in (b) is the Solar Neighborhood stars.

$\bar{L}_X$  ( $\bar{L}_K$ ) the characteristic X-ray (K-band) luminosity of a binary (star), and  $N_X/N_b$  the fraction of binaries being an X-ray-emitting close binary. We follow Paper I to calculate  $L_X$  and  $L_K$  from the same photometry extraction region (i.e., within the half-light circle). Both  $L_X$  and  $L_K$  have been corrected from extinction with the foreground reddening ( $E(B - V)$ ) of Harris (2010 edition). It turns out that the measurement error of  $L_K$  is small (with relative error  $\lesssim 1\%$ ) compared to that in  $L_X$  (with relative error  $\lesssim 30\%$  in most GCs), hence the error in  $L_X/L_K$  is dominated by  $L_X$ . According to Equation (6), we can use the parameter  $L_X/(L_K f_b)$  to diagnose the dynamical interactions of binaries in GCs, which could be regarded as the transformation rate of MS binaries into X-ray-emitting close binaries. We refer to this parameter as the *binary hardness ratio*.

In Figure 1b, we plot  $L_X/(L_K f_b)$  versus the specific encounter rate  $\gamma$ , which is defined as  $\gamma \equiv \Gamma/M_6$ , with the value of  $\Gamma$  adopted from Bahramian et al. (2013), and  $M_6$  is the cluster mass in units of  $10^6 M_\odot$ . The Spearman’s rank correlation coefficient shows a significant positive correlation between these two parameters, with  $r = 0.689$  and  $r = 0.658$  for the dynamically normal and total GCs, while the random correlation p-value is  $p = 0.0002$  and

$p < 0.0001$ , respectively. This clearly supports a dynamical origin of weak X-ray sources in GCs, in particular the dynamically normal ones. We fit these GCs with a power-law function, which gives  $L_X/(L_K f_b) \propto \gamma^{0.65 \pm 0.12}$  (purple line in Figure 1b).

For comparison, we also plot the cases of the NSC and Solar neighborhood in Figure 1b. The NSC is marked by the green crosses, with the upper limit of  $L_X/(L_K f_b)$  varying from  $1.48 \times 10^{29} \text{ erg s}^{-1} L_{K,\odot}^{-1}$  to  $14.8 \times 10^{29} \text{ erg s}^{-1} L_{K,\odot}^{-1}$  ( $f_b$  from 1%–10%). Here, the uncertainty in  $L_X/(L_K f_b)$  is dominated by the poorly constrained  $f_b$  in the NSC. In case of the latter upper limit, the NSC is again consistent with the relation defined by the GCs in Figure 1b.

Due to the collisionless environment, the Solar neighborhood is marked as the magenta horizontal strip in Figure 1b, with  $L_X/(L_K f_b) = (8.6 \pm 1.6) \times 10^{27} \text{ erg s}^{-1} L_{K,\odot}^{-1}$ . Estimate of this value has adopted the X-ray emissivity of Solar neighborhood stars from Sazonov et al. (2006) and Revnivtsev et al. (2007), the mass-to-light ratio for the Solar cylinder of  $M/L_K = 0.34 M_\odot/L_{K,\odot}$  (Just et al. 2015), and the frequency of Solar neighborhood stars in binary or multiple systems of  $46 \pm 2\%$  (Raghavan et al. 2010). If all the primordial binaries in GCs followed the normal stellar evolution path as in the Galactic field

binaries, the GCs should have a similar value of  $L_X/(L_K f_b)$  as that of the Solar neighborhood. However, almost all GCs are located above the magenta strip in Figure 1b, which suggests that the evolution of primordial binaries in GCs had been substantially altered by dynamical interactions. MS binaries have either been transformed into X-ray-emitting close binaries, or been dynamically disrupted, leading to a larger value of  $L_X/(L_K f_b)$  with respect to the field.

#### 4. Testing the Hills-Heggie Law

In Paper I, we found no significant dependence of the abundance of weak X-ray sources (traced by  $L_X/L_K$ ) on  $f_b$  or the cluster central velocity dispersion  $\sigma_c$ . On the other hand,  $f_b$  was found to be anti-correlated with  $\sigma_c$  (Milone et al. 2012). According to the Hills-Heggie law, MS binaries will be gradually exhausted in GCs, and the average stellar kinetic energy plays a vital role in determining whether a MS binary could be dynamically disrupted or be dynamically transformed into X-ray emitting close binaries. Therefore, with the observed binary hardness ratio of GCs, we can test the Hills-Heggie law as in Figure 2, where  $L_X/(L_K f_b)$  was plotted against  $\sigma_c$ <sup>9</sup>. The value of  $\sigma_c$  is adopted from (Harris 2010 edition), which has a relative error  $\lesssim 10\%$  in most GCs. Clearly, there is a positive correlation between  $L_X/(L_K f_b)$  and  $\sigma_c$  in dynamically normal GCs. The Spearman's rank correlation coefficient and random correlation p-value is  $r = 0.654$  and  $p = 0.0018$ , respectively. We fit the dynamically normal GCs with a power-law function, which gives  $L_X/(L_K f_b) \propto \sigma^{1.71 \pm 0.48}$  (purple line in Figure 2). We note that the fitted slope is consistent with a value of 2, which is the case if the binary hardness ratio has a strong dependence on the average stellar kinetic energy ( $E_k \propto \sigma^2$ ).

As self-gravitating systems, GCs are unstable against core collapse without some source of internal energy. Binaries serve as a reservoir of energy in GCs. The Hills-Heggie law predicts that they will support the clusters from collapse, provided that they can be effectively transformed into harder systems through  $b$ - $s$  and  $b$ - $b$  encounters (Hut 1983). This prediction can also be tested with the correlation shown in Figure 2. Note that binaries in core-collapsed GCs exhibit a higher binary hardness ratio than in dynamically normal GCs, which suggests that these systems are running out of their MS binary systems. Indeed, core-collapsed GCs

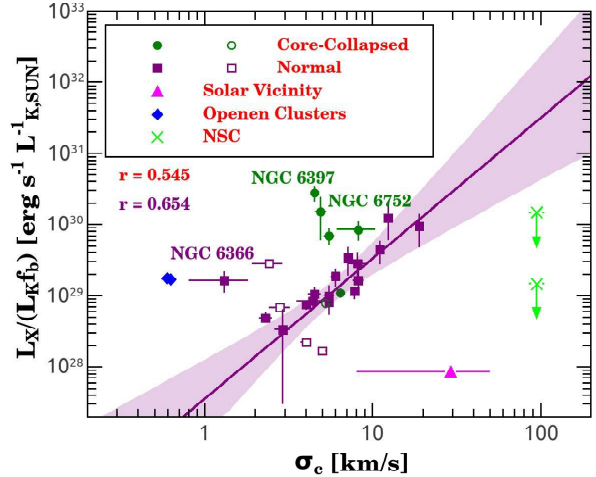


Fig. 2.—  $L_X/(L_K f_b)$  as a function of cluster central velocity dispersion. Color-coded symbols and texts represent the different types of clusters and corresponding correlation coefficients as in Figure 1. The solid lines are the best-fitting functions of dynamically normal GCs (GCs with upper limit were not included in the fit), while the shaded area represent the 95% confidence of linear regression. The magenta up-triangle marks the Solar neighborhood stars, which has a large scatter in  $\sigma$  among stars of different ages (Griv et al. 2009). The blue diamonds represent the two open clusters, with  $\sigma = 0.62 \pm 0.1$  km s<sup>-1</sup> for NGC 6791 (Tofflemire et al. 2014) and  $\sigma = 0.59^{+0.07}_{-0.06}$  km s<sup>-1</sup> for M 67 (Geller et al. 2015).

have systematically lower  $f_b$  than dynamically normal GCs (Milone et al. 2012). The contraction of cluster core will shorten the timescale of binary encounter, thereby boosting the extraction of energy from harder binaries.

Observationally, the hardening of binaries in GCs can also be tested with the luminosity function (LF, in the form of  $dN/d\log L_X \propto L_X^{-\alpha}$ ) of the weak X-ray sources. For example, the dynamically older GCs (with higher central stellar density  $\rho_c$ ) were found to host more bright X-ray sources, and the value of  $\alpha$  was found to be anti-correlated with  $\rho_c$  in GCs (Pooley et al. 2002). Comparing to the Solar neighborhood stars (with  $\alpha \approx 1.12$ , Sazonov et al. (2006)), the power-law slopes of GC-LFs were found to be much flatter (with  $\alpha < 1$ ), which suggests that dynamical interactions are effective in transforming binaries into bright X-ray sources in GCs.

For comparison, we also plot the cases of the NSC, Solar neighborhood and two open clusters (i.e., NGC 6791 and M 67) in Figure 2. The

<sup>9</sup>We emphasize that here  $\sigma_c$  is more suitable than  $\sigma(r)$  in determining the evolution of binaries in GCs, since binaries tend to sink to the cluster core under the effect of mass segregation, where stellar dynamical interactions are more frequent.

NSC and Solar neighborhood were shown as green crosses and magenta up-triangle separately; the two open clusters, with  $L_X/(L_K f_b) = (1.7 \pm 0.2) \times 10^{29} \text{ erg s}^{-1} \text{ M}_{\odot}^{-1}$  for NGC 6791 and  $L_X/(L_K f_b) = 1.76 \times 10^{29} \text{ erg s}^{-1} \text{ M}_{\odot}^{-1}$  for M 67, were plotted as blue diamonds. To obtain these values, we have adopted the X-ray emissivity ( $L_X/L_K$ ) from van den Berg et al. (2013), and the MS binary fraction of  $f_b = 30 \pm 5\%$  for NGC 6791 (Bedin et al. 2008) and  $f_b = 45\%$  for M 67 (Davenport et al. 2010), respectively.

Due to the collisionless environment, although Solar neighborhood stars show larger  $f_b$  and  $\sigma$  than the clusters, their binary hardness ratio is the lowest in Figure 2. For open clusters, they have larger binary hardness ratio than the Solar neighborhood and some of the GCs, but these systems tend to disperse quickly, hence evaporation and mass segregation effects will leave these systems with a large fraction of MS binaries (with  $f_b$  comparable to the Solar neighborhood) and the lowest stellar velocity dispersion. Hence the higher value of  $L_X/(L_K f_b)$  in open clusters is more likely due to the substantial loss of single stars rather than dynamical hardening of MS binaries. In fact, the location of open clusters in Figure 2 is close to NGC 6366, a GC known to suffer from strong tidal stripping (Paust et al. 2009). Notably, the NSC shows a much lower binary hardness ratio than that predicted by the GCs in Figure 2. The NSCS also exhibits a steep LF, with  $\alpha \approx 1.63$  over the luminosity range of  $10^{31-33} \text{ erg s}^{-1}$  (Zhu et al. 2018). The implication of these findings will be addressed in Section 5.

## 5. Discussion: NSC in Context

As the most massive and the densest star cluster in the Milky Way, the NSC offers a unique laboratory for studying stellar dynamics in high stellar velocity dispersion environment, especially under the gravitational influence of the super-massive black hole (SMBH). The X-ray sources detected in the NSC, mainly close binaries with accreting compact objects, may serve as sensitive probes of the stellar dynamics in this dense environment. It is also important to make connection between the NSC and GCs, as the former has been suggested to be assembled, at least in part, by sequential mergers of GCs that spiraled into the deep gravitational well of the Galactic center, due to dynamical friction (Tremaine et al. 1975; Antonini et al. 2012; Antonini 2013; Arca-Sedda & Capuzzo-Dolcetta 2014; Gnedin et al. 2014). Alternatively, the NSC might be formed through continuous *in-situ* star formation, supplied by gas inflow that is driven by some

still poorly understood processes (Milosavljević 2004; Emsellem & van de Ven 2008).

In Figure 1, we found that the NSC is compatible with the correlations defined by the GCs, which may imply for a common origin for the weak X-ray sources in GCs and the NSC. Indeed, there are many similarities between NSC and GCs in the populations of X-ray sources. For example, about a dozen bright transient X-ray sources, mainly BH-LMXBs and NS-LMXBs, have been detected in the NSC (Muno et al. 2005; Degenaar et al. 2015). The spatial distribution of these transient sources was found to be scaled with the square of the stellar density profile ( $\rho^2(r)$ ) of the NSC, strongly suggesting a dynamical origin (Zhu et al. 2018). On the other hand, the weak and steady X-ray sources, i.e., CVs, show a spatial distribution that matches well with the stellar density profile ( $\rho(r)$ ; Zhu et al. 2018). At first sight, these findings may suggest a universal scenario for forming X-ray sources in dense stellar environments including GCs and the NSC: a dynamical origin is responsible for the over-abundance of NS-LMXBs or BH-LMXBs, while CVs are mainly descendant from the primordial binaries that have been modified by stellar dynamical interactions.

Nevertheless, the stellar velocity dispersion in the NSC,  $\sigma \sim 100 \text{ km s}^{-1}$ , is about one order of magnitude higher than that in GCs, which suggests a much shorter watershed orbital period ( $P_w$ ) for binaries in the NSC according to the Hills-Heegie law. Furthermore, the stars used to quantify  $\sigma$  in the NSC are typically younger and more massive (with an average mass of  $\sim 1.5 - 3 \text{ M}_{\odot}$ ; Schödel et al. 2007) than the older stellar populations represented by the X-ray sources. With these conditions taken into account, we estimate  $P_w \sim 1 - 4$  days for binaries with a stellar mass of  $1 \text{ M}_{\odot}$  in the NSC. Such a watershed period is much shorter than the typical period of ABs ( $P_{orb} \sim 10$  days; Eker et al. 2008), indicating that even close binaries like ABs could be disrupted dynamically in the NSC. On the other hand,  $P_w$  is comparable to the maximum period of CVs and LMXBs (Ritter & Kolb 2003, 7.23 edition), thus formation of these systems through *b-s/b-b* encounters are inefficient in the NSC.

For the BH-LMXBs and NS-LMXBs in the NSC, Generozov et al. (2018) suggested that they could be formed by tidal capture of stars by BHs and NSs. Alternatively, NS-LMXBs and their descendant, MSPs, could be inherited from GCs having spiralled into the Galactic center (Arca-Sedda et al. 2018). For the CVs, their abundance was found to be slightly higher in the NSC with respect to the field CV population over the same luminosity range (Zhu et al. 2018). According to the Hills-



Heggie law, this feature is inconsistent with the in-situ star formation scenario of the NSC, since most of the primordial binaries would have been disrupted dynamically before they can otherwise evolve into CVs. However, if most CVs in the NSC are inherited from the dense cores of GCs, their present-day abundance would depend on the evolutionary phase of the parent GCs (Arca-Sedda et al. 2018). The dynamically older GCs tend to have a high abundance of weak X-ray sources (Paper I), and the host galaxy’s tidal field will also accelerate the evolution of GCs (Gnedin et al. 1999).

The NSC was found to show a much lower  $L_X/(L_K f_b)$  than predicted for its  $\sigma$  (Figure 2). We suggest that this discrepancy may be caused by the different population of X-ray sources in GCs and NSC, which is ultimately related to the difference in the watershed period (velocity) that distinguishes soft/hard binaries, i.e.,  $P_w \approx 5000$  days in GCs versus  $P_w \approx 1 - 4$  days in the NSC. As discussed in the above, the small- $P_w$  environment of the NSC disfavors the formation of ABs, and in the meantime tends to accelerate the evolution of CVs, driving them towards smaller  $P_{\text{orb}}$ , lower mass transfer rates and lower X-ray luminosities (Patterson 1984; Townsley & Gänsicke 2009; Patterson 2011). This in turn results in a lower binary hardness ratio in the NSC.

Alternatively, the low  $L_X/(L_K f_b)$  in the NSC might be partially explained by the presence of the SMBH, also known as Sgr A\*. The NSC stars are expected to be heated when they come close to the SMBH, as a result, the hardening of binaries is inefficient and binaries are more likely to be disrupted. Such an effect has been predicted by the simulations of Hopman (2009).

## 6. Conclusion

To bring isolated stars (or loosely bounded binaries) together to form X-ray sources, the fundamental issue is how to dissipate the stars’ kinetic energy (or binary bounding energy) effectively. Early studies of stellar dynamical interactions in dense stellar environments have provided various scenarios for solving this problem. In this work, we strengthen the importance of  $b$ - $s$  and  $b$ - $b$  encounters as an effective formation mechanism for X-ray sources in GCs. We have demonstrated a tight correlation between the MS binary encounter rate ( $\Gamma_b$ ) and the total luminosity (hence number) of weak X-ray sources in 30 Galactic GCs. Using a physical parameter  $L_X/(L_K f_b)$  for these GCs, we have verified the Hills-Heggie law, which states that stellar encounters involving hard binaries make them harder, whereas encounters involving soft binaries drive them softer

and eventually disrupted. Applying the Hills-Heggie law to the dynamic environment of the NSC, we argue that both the dynamical and primordial channels of CV formation are suppressed, and that a large fraction of the weak X-ray sources detected therein might have been inherited from GCs captured into the Galactic center.

We thank the anonymous referee for valuable comments that help improve our manuscript. This work is supported by the National Key R&D Program of China No. 2017YFA0402600, the National Science Foundation of China under grants 11525312, 11133001, 11333004 and 11303015.

## REFERENCES

- Antonini, F., Capuzzo-Dolcetta, R., Mastrobuono-Battisti, A., & Merritt, D. 2012, *ApJ*, 750, 111
- Antonini, F. 2013, *ApJ*, 763, 62
- Arca-Sedda, M., & Capuzzo-Dolcetta, R. 2014, *MNRAS*, 444, 3738
- Arca-Sedda, M., Kocsis, B., & Brandt, T. D. 2018, *MNRAS*,
- Bacon, D., Sigurdsson, S., Davis, M. B., 1996, *MNRAS*, 281, 830
- Bahramian, A., Heinke, C.O., Sivakoff, G.R., & Gladstone, J.C. 2013, *ApJ*, 766, 136
- Bedin, L. R., Salaris, M., Piotto, G., et al. 2008, *ApJ*, 679, L29
- Chatterjee, S., Rasio, F. A., Sills, A., & Glebbeek, E. 2013, *ApJ*, 777, 106
- Cheng, Z., Li, Z., Xu, X., & Li, X. 2018, *ApJ*, 858, 33
- Clark, G. W. 1975, *ApJ*, 199, L143
- Davies, M. B., 2002, *ASPC*, 263, 17
- Davenport, J. R. A., & Sandquist, E. L., 2010, *ApJ*, 711, 559
- Degenaar, N., Wijnands, R., Miller, J. M., et al. 2015, *Journal of High Energy Astrophysics*, 7, 137
- de Grijs, R., Li, C., Zheng, Y., et al. 2013, *ApJ*, 765, 4
- Duquennoy, A., Mayor, M., 1991, *A&A*, 248, 485
- Eker, Z., Ak, N. F., Bilir, S., et al. 2008, *MNRAS*, 389, 1722



TABLE 1  
BASIC PROPERTIES OF STAR CLUSTERS

Name — (1)	$\Gamma$ — (2)	$f_b$ % (3)	$\Gamma_b$ — (4)	$\gamma$ — (5)	$\sigma$ $\text{km s}^{-1}$ (6)	$L_X$ $10^{32} \text{ erg s}^{-1}$ (7)	$L_K$ $10^4 L_{K,\odot}$ (8)	$L_X/(L_K f_b)$ $10^{28} \text{ erg s}^{-1} L_{K,\odot}^{-1}$ (9)
Normal GCs:								
NGC 104	$1000^{+150}_{-130}$	$1.8 \pm 0.6$	$180^{+66}_{-65}$	$840^{+130}_{-110}$	$11.0 \pm 0.3$	$58.9^{+7.7}_{-8.6}$	74.6	$44^{+16}_{-16}$
NGC 288	$0.77^{+0.28}_{-0.21}$	$11.2 \pm 0.8$	$0.86^{+0.32}_{-0.24}$	$7.6^{+2.8}_{-2.0}$	$2.9 \pm 0.3$	$1.3^{+1.2}_{-1.2}$	3.4	$3.3^{+3.1}_{-3.0}$
NGC 3201	$7.2^{+3.6}_{-2.3}$	$12.2 \pm 0.6$	$8.8^{+4.4}_{-2.8}$	$37^{+18}_{-12}$	$5.0 \pm 0.2$	$< 1.5$	7.2	$< 1.7$
NGC 5024	$35^{+12}_{-10}$	$6.2 \pm 0.6$	$22.0^{+8.0}_{-6.3}$	$58^{+20}_{-16}$	$4.4 \pm 0.9$	$12.1^{+2.6}_{-2.6}$	23.1	$8.5^{+2.0}_{-2.0}$
NGC 5272	$194^{+33}_{-18}$	$3.4 \pm 0.6$	$66^{+16}_{-13}$	$269^{+46}_{-25}$	$5.5 \pm 0.3$	$9.1^{+3.1}_{-2.6}$	33.0	$8.2^{+3.1}_{-2.8}$
NGC 5286	$458^{+58}_{-61}$	$1.8 \pm 0.6$	$82^{+29}_{-30}$	$723^{+92}_{-96}$	$8.1 \pm 0.1$	$13.5^{+3.6}_{-2.6}$	26.1	$29^{+12}_{-11}$
NGC 5904	$164^{+39}_{-30}$	$2.2 \pm 0.6$	$36^{+13}_{-12}$	$243^{+57}_{-45}$	$5.5 \pm 0.4$	$5.1^{+1.4}_{-0.8}$	22.8	$10.1^{+3.9}_{-3.2}$
NGC 5927	$68^{+13}_{-10}$	$3.2 \pm 0.6$	$21.8^{+5.8}_{-5.3}$	$254^{+47}_{-38}$	...	$4.9^{+1.2}_{-0.8}$	17.3	$8.8^{+2.8}_{-2.2}$
NGC 6093	$532^{+59}_{-69}$	$1.2 \pm 0.6$	$64^{+33}_{-33}$	$1340^{+150}_{-170}$	$12.4 \pm 0.6$	$23.7^{+1.4}_{-1.8}$	16.1	$123^{+62}_{-62}$
NGC 6121	$27^{+12}_{-10}$	$12.2 \pm 0.8$	$33^{+14}_{-12}$	$177^{+76}_{-63}$	$4.0 \pm 0.2$	$5.3^{+0.0}_{-0.7}$	5.8	$7.5^{+0.5}_{-1.1}$
NGC 6144	$3.1^{+1.1}_{-0.9}$	$9.6 \pm 0.6$	$3.0^{+1.0}_{-0.8}$	$28.3^{+9.6}_{-7.7}$	...	$5.0^{+1.4}_{-0.8}$	4.7	$11.0^{+3.1}_{-1.9}$
NGC 6205	$69^{+18}_{-15}$	$1.4 \pm 0.6$	$9.7^{+4.9}_{-4.6}$	$130^{+34}_{-28}$	$7.1 \pm 0.4$	$9.2^{+0.6}_{-0.7}$	19.4	$34^{+15}_{-15}$
NGC 6218	$13.0^{+5.4}_{-4.0}$	$7.4 \pm 0.6$	$9.6^{+4.1}_{-3.1}$	$77^{+32}_{-24}$	$4.5 \pm 0.4$	$4.0^{+1.0}_{-0.8}$	5.1	$10.6^{+2.7}_{-2.3}$
NGC 6341	$270^{+30}_{-29}$	$2.2 \pm 0.6$	$59^{+18}_{-17}$	$695^{+77}_{-75}$	$6.0 \pm 0.4$	$5.4^{+0.5}_{-0.5}$	13.2	$18.6^{+5.4}_{-5.3}$
NGC 6352	$6.7^{+1.7}_{-1.3}$	$13.8 \pm 0.8$	$9.3^{+2.4}_{-1.9}$	$86^{+22}_{-17}$	...	$4.1^{+0.8}_{-0.9}$	6.1	$4.9^{+1.0}_{-1.1}$
NGC 6362	$4.6^{+1.5}_{-1.0}$	$9.2 \pm 0.6$	$4.2^{+1.4}_{-1.0}$	$37^{+12}_{-9}$	$2.8 \pm 0.4$	$< 3.9$	6.1	$< 6.9$
NGC 6366	$5.1^{+2.8}_{-1.8}$	$18.4 \pm 1.4$	$9.5^{+5.1}_{-3.3}$	$129^{+69}_{-44}$	$1.3 \pm 0.5$	$3.2^{+1.0}_{-1.0}$	1.1	$16.3^{+5.5}_{-5.2}$
NGC 6388	$900^{+240}_{-210}$	$1.6 \pm 0.8$	$144^{+81}_{-80}$	$770^{+200}_{-180}$	$18.9 \pm 0.8$	$88.8^{+1.7}_{-2.8}$	58.4	$95^{+48}_{-48}$
NGC 6535	$0.39^{+0.40}_{-0.20}$	$6.6 \pm 1.8$	$0.26^{+0.27}_{-0.14}$	$24^{+24}_{-12}$	$2.4 \pm 0.5$	$< 1.2$	0.6	$< 28.7$
NGC 6637	$90^{+36}_{-18}$	$6.0 \pm 0.6$	$54^{+22}_{-12}$	$390^{+160}_{-80}$	...	$16.6^{+5.6}_{-3.7}$	16.0	$17.3^{+6.1}_{-4.3}$
NGC 6656	$78^{+32}_{-26}$	$4.4 \pm 0.6$	$34^{+15}_{-12}$	$153^{+63}_{-51}$	$7.8 \pm 0.3$	$10.6^{+0.3}_{-2.1}$	20.8	$11.6^{+1.6}_{-2.7}$
NGC 6809	$3.2^{+1.4}_{-1.0}$	$8.0 \pm 0.6$	$2.6^{+1.1}_{-0.8}$	$15.0^{+6.4}_{-4.6}$	$4.0 \pm 0.3$	$< 1.3$	7.0	$< 2.2$
NGC 6838	$1.5^{+0.2}_{-0.1}$	$23.4 \pm 1.4$	$3.4^{+0.4}_{-0.4}$	$41.5^{+4.1}_{-3.9}$	$2.3 \pm 0.2$	$2.7^{+0.5}_{-0.4}$	2.3	$4.9^{+1.0}_{-0.7}$
NGC 7089	$518^{+78}_{-71}$	$2.6 \pm 0.6$	$135^{+37}_{-36}$	$626^{+94}_{-86}$	$8.2 \pm 0.6$	$14.2^{+6.4}_{-4.0}$	33.2	$16.5^{+8.3}_{-6.0}$
Core-Collapsed GCs:								
NGC 362	$740^{+140}_{-120}$	$4.0 \pm 0.6$	$294^{+70}_{-64}$	$1540^{+290}_{-250}$	$6.4 \pm 0.3$	$9.2^{+0.3}_{-0.5}$	20.6	$11.1^{+1.7}_{-1.8}$
NGC 6397	$840^{+180}_{-180}$	$2.4 \pm 0.6$	$20.2^{+6.7}_{-6.7}$	$920^{+200}_{-200}$	$4.5 \pm 0.2$	$13.3^{+0.5}_{-0.5}$	2.0	$281^{+71}_{-71}$
NGC 6541	$386^{+95}_{-63}$	$2.0 \pm 0.6$	$77^{+30}_{-26}$	$750^{+180}_{-120}$	$8.2 \pm 2.1$	$22.6^{+0.1}_{-0.1}$	13.3	$85^{+26}_{-26}$
NGC 6681	$1040^{+270}_{-190}$	$3.8 \pm 0.6$	$400^{+120}_{-100}$	$7300^{+1800}_{-1400}$	$5.2 \pm 0.5$	$< 1.4$	4.6	$< 7.9$
NGC 6752	$400^{+180}_{-130}$	$1.0 \pm 0.6$	$40^{+30}_{-27}$	$1610^{+730}_{-500}$	$4.9 \pm 0.4$	$11.1^{+0.4}_{-0.4}$	7.3	$153^{+92}_{-92}$
NGC 7099	$320^{+120}_{-80}$	$2.4 \pm 0.6$	$78^{+36}_{-28}$	$1680^{+640}_{-420}$	$5.5 \pm 0.4$	$8.7^{+0.6}_{-0.6}$	5.2	$70^{+18}_{-18}$
Galactic Nuclear Star Cluster (with parameters obtained within $r \leq 100''$ ):								
NSC	$25600^{+7700}_{-7700}$	$1.0 - 10.0$	$2560 - 25600$	$4200^{+1200}_{-1200}$	$90 - 100$	$< 1374$	$1194 \pm 339$	$< 14.8 - 148$

NOTE.—(1) Target name; (2) Encounter rate adopted from Bahramian et al. (2013), for the NSC, the encounter rates are estimated in this work (see Section 3); (3) Main sequence binary fraction in units of percentage (Milone et al. 2012), the binary fraction of the NSC is estimated in this work (see Section 3); (4) Binary-single and binary-binary encounter rate; (5) The specific encounter rate; (6) Cluster velocity dispersion in units of  $\text{km s}^{-1}$  (Harris 2010 edition); (7) 0.5-8 keV cumulative luminosity in units of  $10^{32} \text{ erg s}^{-1}$ ; (8) K-band luminosity in units of  $10^4 L_{K,\odot}$ . For the NSC, a cumulative mass of  $(609 \pm 97) \times 10^6 M_\odot$  within  $r \leq 100''$  is converted into the K-band luminosity using a mass-to-light ratio of  $M/L_K = 0.51 \pm 0.12 M_\odot/L_{K,\odot}$  (Fritz et al. 2016); (9) Binary hardness ratio, in units of  $10^{28} \text{ erg s}^{-1} L_{K,\odot}^{-1}$ .

- Emsellem, E., & van de Ven, G. 2008, *ApJ*, 674, 653
- Fabian, A. C., Pringle, J. E., & Rees, M. J. 1975, *MNRAS*, 172, 15P
- Fregeau, J. M., Cheung, P., Portegies Zwart, S. F., & Rasio, F. A. 2004, *MNRAS*, 352, 1
- Fritz, T. K., Chatzopoulos, S., Gerhard, O., et al. 2016, *ApJ*, 821, 44
- Geller, A. M., Latham, D. W., Mathieu, R. D., 2015, *ApJ*, 150, 97
- Generozov, A., Stone, N. C., Metzger, B. D., & Ostriker, J. P. 2018, arXiv:1804.01543
- Gnedin, O. Y., Lee, H. M., & Ostriker, J. P. 1999, *ApJ*, 522, 935
- Gnedin, O. Y., Ostriker, J. P., & Tremaine, S. 2014, *ApJ*, 785, 71
- Griv, E., Gedalin, M., & Eichler, D. 2009, *AJ*, 137, 3520
- Güdel, M. 2004, *A&A Rev.*, 12, 71
- Hailey, C. J., Mori, K., Perez, K., et al. 2016, *ApJ*, 826, 160
- Hailey, C. J., Mori, K., Bauer, F. E., et al. 2018, *Nature*, 556, 70
- Harris, W. E. 1996(2010 edition), *AJ*, 112, 1487.
- Heggie, D. C., 1975, *MNRAS*, 173, 729
- Heggie, D. C., Hut, P., & McMillan, S. L. W. 1996, *ApJ*, 467, 359
- Heinke, C. O. 2010, in *AIP Conf. Proc.* 1314, International Conference of Binaries: In celebration of Ron Webbink's 65th Birthday (Melville, NY: AIP), 135
- Hills, J. G., 1975, *AJ*, 80, 809
- Hills, J. G., 1976, *MNRAS*, 175, 1P
- Hoffer, J. B., 1983, *AJ*, 88, 1420
- Hopman, C. 2009, *ApJ*, 700, 1933
- Hut, P., 1983, *ApJ*, 272, L29
- Hut, P., McMillan, S., Romani, R. W., 1992, *ApJ*, 389, 527
- Hut, P., McMillan, S., Goodman, J., et al. 1992, *PASP*, 104, 981
- Hut, P., 1993, *ApJ*, 403, 256
- Ivanova, N., Heinke, C. O., Rasio, F. A., Taam, R. E., et al. 2006, *MNRAS*, 372, 1043
- Ivanova, N., Heinke, C. O., Rasio, F. A., et al. 2008, *MNRAS*, 386, 553
- Ji, J., Bregman, J. N., 2015, *ApJ*, 807, 32
- Jordán, A., et al. 2004, *ApJ*, 613, 279
- Jordán, A., et al. 2007, *ApJ*, 671, 117
- Just, A., Fuchs, B., Jahreiß, H., et al. 2015, *MNRAS*, 451, 149
- Katz, J. I. 1975, *Nature*, 253, 698
- Maxwell, J. E., Lugger, P. M., Cohn, H. N., et al. 2012, *ApJ*, 756, 147
- Muno, M. P., Pfahl, E., Baganoff, F. K., et al. 2005, *ApJ*, 622, L113
- Mikkola, S., 1983, *MNRAS*, 203, 1107
- Mikkola, S., 1984, *MNRAS*, 207, 115
- Mikkola, S., 1984, *MNRAS*, 208, 75
- Milone, A. P., Piotto, G., Bedin, L. R., et al. 2012, *A&A*, 540, 16
- Milosavljević, M. 2004, *ApJ*, 605, L13
- Patterson, J. 1984, *ApJS*, 54, 443
- Patterson, J. 2011, *MNRAS*, 411, 2695
- Paust, N. E. Q., Aparicio, A., Piotto, G., et al. 2009, *AJ*, 137, 246
- Peacock, M. B., et al. 2009, *MNRAS*, 392, 55
- Pooley, D., Lewin, W. H. G., Verbunt F., et al. 2002, *ApJ*, 573, 184
- Pooley, D., Lewin, W. H. G., Anderson, S. F., et al. 2003, *ApJ*, 591, L131
- Pooley, D., & Hut, P. 2006, *ApJ*, 646, 143
- Raghavan, D., McAlister, H. A., Henry, T. J., et al. 2010, *ApJS*, 190, 1
- Rasio, F. A., Pfahl, E. D., & Rappaport, S. 2000, *ApJ*, 532, L47
- Reis, R. C., Wheatley, P. J., Gänsicke, B. T., & Osborne, J. P. 2013, *MNRAS*, 430, 1994

- Revnivtsev, M., Churazov, E., Sazonov, S., Forman, W., & Jones, C. 2007, *A&A*, 473, 783
- Ritter, H., & Kolb, U. 2003, *A&A*, 404, 301
- Sazonov, S., Revnivtsev, M., Gilfanov, M., et al. 2006, *A&A*, 450, 117
- Schödel, R., Eckart, A., Alexander, T., et al. 2007, *A&A*, 469, 125
- Sivakoff, G. R., Jordan, A., Sarazin, C. L., et al. 2007, *ApJ*, 660, 1246
- Sollima, A., Beccari, G., Ferraro, F. R., et al. 2007, *MNRAS*, 380, 781
- Sutantyo, W. 1975, *A&A*, 44, 227
- Tremaine, S. D., Ostriker, J. P., & Spitzer, L., Jr. 1975, *ApJ*, 196, 407
- Tofflemire, B.M., Gosnell, N. M., et al. 2014, *AJ* 148, 61
- Townsley, D. M., & Gänsicke, B. T. 2009, *ApJ*, 693, 1007
- van den Berg, M., Verbunt, F., Tagliaferri, G., et al. 2013, *ApJ*, 770, 98
- Verbunt, F., & Hut, P. 1987, in: *The Origin and Evolution of Neutron Stars IAU Symp.125*, eds. D.J. Helfand and J.H. Huang, Reidel, p.187
- Verbunt, F. 2003, *New Horizons in Globular Cluster Astronomy*, 296, 245
- Zhu, Z., Li, Z., & Morris, M. R. 2018, *ApJS*, 235, 26
- Xu, X.-j., & Li, Z. 2018, *ApJ*, 856, 77